RESEARCH ARTICLE

Reservoir Characteristics and Controlling Factors of the Upper Permian Changxing Formation Reef-Shoal Carbonate Reservoirs in the Huanglongchang Structure, Eastern Sichuan Basin

Liao Pan[1], **Qirong Qin**[1], **Shilin Wang**[1,*], **Hening Li**[1] **and Mei Luo**[1]

[1] School of Geoscience and Technology, Southwest Petroleum University, Chengdu 610500, China

Abstract

The Upper Permian Changxing Formation reef-shoal carbonates in the Huanglongchang Structure, eastern Sichuan Basin, are important gas reservoirs, yet their characteristics and controlling mechanisms remain poorly understood. We integrated 481 core samples and 126 cast thin sections from 8 wells with logging, petrophysical, and structural data to characterize reservoir properties and controls. The results show that: (1) Reservoirs are dominated by oolitic, reef breccia, and rudstone dolomites, with secondary dissolution pores as the main storage space. They exhibit low porosity, low permeability, and strong heterogeneity, with porosity of 4%–12% and permeability of 0.1–10 mD. (2) The thermogenic dry gas contains 92.86%–97.41% methane. $CaCl_2$-type formation water has an average TDS of 110.15 g/L, indicating a strongly confined accumulation environment. (3) Platform-margin reef-shoal facies are most favorable for reservoir development, particularly back-reef shoals, with an average effective porosity of 8.75%. (4) Multi-stage dolomitization and dissolution are the principal constructive diagenetic processes. Burial dolomitization creates a compaction-resistant intercrystalline pore framework, while karstification and burial dissolution enlarge storage space. Yanshanian and Himalayan fractures further enhance permeability, with fracture intensity increasing toward structural highs and greater fold curvature. Therefore, overlap zones of platform-margin reef-shoal bodies and structural highs are most favorable for high-quality reservoirs. These results establish a coupled model of "sedimentary facies constraint–diagenetic modification–tectonic fracture enhancement" and provide guidance for reef gas exploration around the Kaijiang-Liangping Trough.

Keywords: Northeastern Sichuan Basin, Huanglongchang structure, Changxing Formation, Reservoir Characteristics, Controlling Factors.

Submitted: 01 July 2026
Revised: 18 August 2026
Accepted: 21 August 2026
Published: 30 September 2026

Vol. 3, **No.** 1, 2027.
10.62762/JGEE.2026.460493

***Corresponding author:**
✉ Shilin Wang
ybybwsl@163.com

Citation
Pan, L., Qin, Q., Wang, S., Li, H., & Luo, M. (2026). Reservoir Characteristics and Controlling Factors of the Upper Permian Changxing Formation Reef-Shoal Carbonate Reservoirs in the Huanglongchang Structure, Eastern Sichuan Basin. *Journal of Geo-Energy and Environment*, 3(1), 28–48.

© 2026 by the Authors. Published by Institute of Central Computation and Knowledge. This is an open access article under the CC BY license (https://creativecommons.org/licenses/by/4.0/).

1 Introduction

Carbonate reef-shoal reservoirs are among the most important hydrocarbon reservoirs globally, accounting for approximately 30% of the world's oil and gas reserves and production. Since the mid-twentieth century, extensive studies have established the fundamental framework for carbonate reef-shoal sedimentology and reservoir characterization. Wilson [1] first proposed the classic carbonate platform facies model, which systematically delineated reef facies belts and clarified the relationships among reef growth, sea-level changes, water energy conditions, and biological community evolution. Schlager [2] further advanced the conceptual framework for carbonate reservoir analysis by integrating sequence stratigraphy with sedimentary facies models, demonstrating how sea-level changes, accommodation space, and depositional geometry collectively govern carbonate platform architecture and the spatial distribution of reservoir-prone facies.

In recent decades, significant progress has been made in international carbonate reservoir research, particularly in the characterization of complex reef architectures and the quantitative evaluation of reservoir heterogeneity. Noyahr et al. [3] developed a high-resolution reservoir model based on facies and sequence stratigraphy for the Devonian South Swan Hills atoll reef in Alberta, Canada, revealing the complex internal geometry of reef reservoirs controlled by relative sea-level fluctuations. Janjuhah et al. [4] investigated the Miocene carbonate platforms in Central Luconia, offshore Malaysia, which contain 60% of Malaysia's gas reserves, and demonstrated that microporosity developed within platform-interior and platform-margin facies plays a significant role in controlling reservoir quality and gas storage capacity, with implications for exploration and development of similar carbonate platform systems. Additionally, advanced technologies such as seismic attribute analysis, spectral decomposition, and dynamic modeling have been widely applied to carbonate reservoir characterization, significantly improving reservoir prediction accuracy and development efficiency.

The Sichuan Basin hosts a series of large marine carbonate gas fields, among which the Puguang sour gas field in northeastern Sichuan represents the largest gas discovery in the Paleozoic marine strata of China, with its reservoir development and accumulation conditions thoroughly characterized by integrated geological, geochemical, and diagenetic analyses [5]. The Upper Permian Changxing Formation contains carbonate deposits of reef-shoal facies, which serve as the primary gas-bearing interval in eastern Sichuan [6, 7]. Since the discovery of the first reef-type gas reservoir in eastern Sichuan in 1974, multiple medium-to-large reef gas reservoirs, including the Puguang, Luojiazhai, Dukouhe, and Yuanba gas fields, have been discovered along the platform margin of the Kaijiang-Liangping Trough, forming a prominent marine reef-shoal gas accumulation belt in China with total reserves exceeding 2000×10^8 m^3 [8].

Over the past decades, domestic scholars have made remarkable achievements in the study of Changxing Formation reef reservoirs. Wang et al. [9] first recognized the controlling effect of the Kaijiang-Liangping Trough on reef distribution, demonstrating that platform-margin facies belts along the trough margin are the most favorable areas for reef development. Ma et al. [7] systematically analyzed the reef-shoal characteristics of the Changxing Formation in the Daxian-Xuanhan area and established the relationship between sedimentary facies and reservoir quality. Recent studies have further revealed the complex diagenetic evolution of Changxing Formation reservoirs, particularly the mechanisms of dolomitization and hydrothermal dissolution and their impacts on reservoir quality. Zuo et al. [10] established four types of platform-margin belt development models on both sides of the Kaijiang-Liangping Trough, providing a theoretical basis for reef prediction in different structural settings.

The Huanglongchang Structure is tectonically located in the southern Shuangshimiao Structural Group of the central uplift and steep structural belt in eastern Sichuan [9, 11]. Situated adjacent to the eastern shelf margin of the Kaijiang-Liangping Trough, this structure possesses favorable sedimentary and tectonic conditions for reef reservoir development, making it a critical block for progressive hydrocarbon exploration of the Changxing Formation reef reservoirs in northeastern Sichuan Basin [12]. Previous studies have demonstrated that the Changxing Formation reef-shoal gas reservoirs in the complex tectonic area of eastern Sichuan are controlled by the interplay of platform-margin sedimentary facies, multi-stage dolomitization, and structural trapping conditions [13], providing a theoretical foundation for understanding the hydrocarbon accumulation mechanism of the Huanglongchang gas reservoir.

Previous studies on the Huanglongchang area

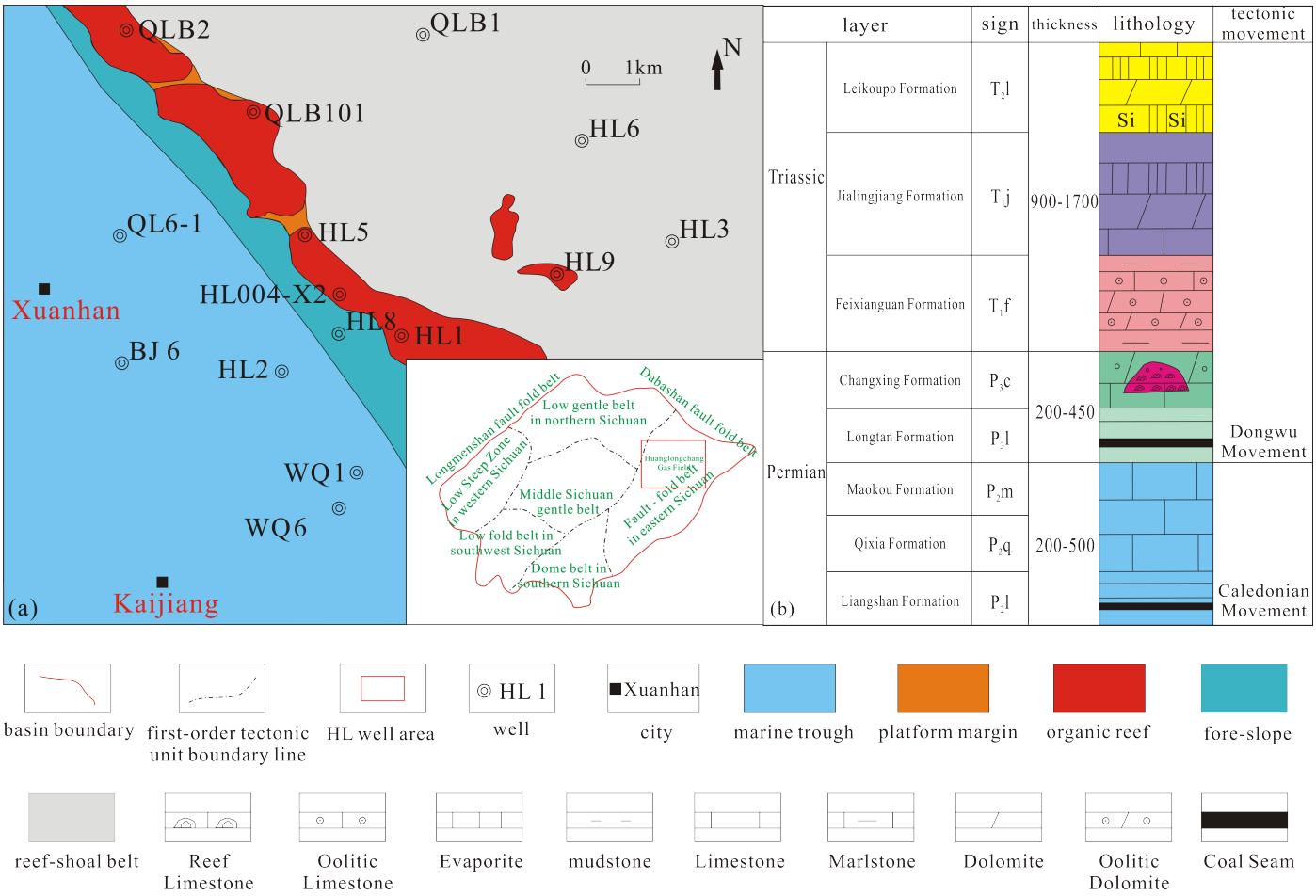


Figure 1. (a) Tectonic location, well distribution and sedimentary facies of the study area; (b) Stratigraphic column from Liangshan Formation to Leikoupo Formation.

have primarily focused on basic geological characteristics. Liu et al. [11] first confirmed the existence of platform-margin reefs in the Huanglongchang Structure through core analysis and proposed a preliminary method for predicting hidden reefs. Zhang et al. [12] described the basic reservoir characteristics of the Changxing Formation in this area and identified dolomitization as a key diagenetic process controlling reservoir development. Zhao et al. [14], working in the adjacent Longhuichang-Tieshan area of northeastern Sichuan Basin, further characterized the seismic-geological signatures and gas reservoir distribution of Changxing Formation biogenic reefs, providing a regional comparative framework for understanding similar reef reservoirs. Recent work by Li et al. [15] further classified the dolomite types in the Huanglongchang area into five categories based on petrological and geochemical characteristics, revealing a complex multi-stage dolomitization history.

Nevertheless, despite these advances, systematic investigations of the Changxing Formation reservoirs in the Huanglongchang Structure remain inadequate. Several critical issues still need to be addressed: (1) fine-scale characterization of reservoir lithology, physical properties, and logging responses is still insufficient, leading to uncertainties in reservoir identification and evaluation; (2) the quantitative relationship between different sedimentary microfacies and reservoir quality has not been clearly established, hindering the prediction of favorable reservoir zones; (3) the coupled reservoir-controlling mechanisms among sedimentary facies, diagenesis, tectonic setting, and fracture distribution have not been thoroughly clarified; and (4) the spatial distribution pattern of high-quality reservoirs and their controlling factors remain poorly understood, thereby restricting precise exploration and efficient development of reef gas reservoirs in this block.

In this study, reservoir samples from the Changxing Formation in the Huanglongchang area were investigated. Thin-section petrography, drilling data, and well logging datasets were comprehensively utilized to systematically characterize reservoir

lithology, physical properties, and electrical responses. The coupled controls of sedimentary facies, diagenesis, and tectonism on reservoir quality were analyzed to clarify the reservoir-controlling mechanism and to provide geological support for further exploration and development of reef gas reservoirs in the study area.

2 Geological Setting

The study area, the Huanglongchang Structure, is located in the southern part of the Shuangshimiao Structural Belt within the central uplift and steep structural zone of the eastern Sichuan Fold Belt, lying in the core of the natural gas enrichment belt in the northeastern Sichuan Basin [9, 11] (Figure 1(a)). It is bounded by the Dukouhe Structure to the north, the Qilixia Structure to the northwest, and the Luojiazhai buried structure to the east, and is adjacent to the intra-platform zone to the south. Eight key wells (HL1, HL2, HL3, HL5, HL5-C1, HL8, HL9, and HL10), distributed across structural highs, axial zones, and limb positions, provide sufficient data for this study.

The stratigraphic sequence from the Upper Permian to the Middle Triassic in the study area is divided into six formations, in ascending order (Figure 1(b)): the Liangshan Formation, Wujiaping Formation, Changxing Formation, Feixianguan Formation, Jialingjiang Formation, and Leikoupo Formation. The Liangshan Formation is dominated by carbonaceous shale and silty shale intercalated with thin-bedded limestone; the Wujiaping Formation consists of open-platform micritic limestone and bioclastic limestone; the Changxing Formation (the target interval) is characterized by platform-margin reef-shoal deposits; the Feixianguan Formation acts as the direct cap rock; and the Jialingjiang and Leikoupo formations are composed of evaporative-platform dolomite and gypsiferous mudstone with superior sealing capacity. The strata are generally in conformable contact, while the Liangshan Formation rests disconformably on the underlying strata, and the top of the Leikoupo Formation has undergone tectonic uplift and erosion.

Controlled by the Emeishan rifting during the Changxing Age of the Late Permian, the Huanglongchang area was situated in the eastern shelf-margin transition zone of the Kaijiang-Liangping Trough. The Changxing Formation is dominated by platform-margin facies, within which the principal sedimentary microfacies include reef core, back-reef shoal, fore-reef shoal, and fore-reef slope. The reef-core and back-reef-shoal microfacies are dominated by algal dolomite, dissolution-modified dolomite, and fine-crystalline dolomite; the fore-reef-shoal microfacies is dominated by bioclastic dolomite; and the fore-reef-ramp microfacies is mainly composed of micritic and argillaceous dolomite [6, 7].

The study area has experienced multi-stage tectonic movements, including the Indosinian, Yanshanian, and Himalayan orogenies. The basic structural prototype was formed during the Indosinian movement, and the structural framework was finalized by strong compression during the Yanshanian movement. The Himalayan movement resulted in intense folding and faulting, promoting the development of abundant tectonic fractures that effectively enhanced reservoir physical properties. Reactivation of basement faults triggered extensional rifting and produced the alternating sedimentary framework of carbonate platforms and troughs, which controlled the spatial distribution of reef-shoal deposits and reservoir development in the Changxing Formation [9].

3 Materials and Methods

3.1 Data Sources

This study focuses on the Upper Permian Changxing Formation reef-shoal reservoirs in the Huanglongchang Structure, northeastern Sichuan Basin. A total of 481 core samples were collected from continuous full-coring intervals of eight key wells (HL1, HL2, HL3, HL5, HL5-C1, HL8, HL9, and HL10), covering structural highs, fold axial zones, and structural limbs to ensure representative sampling. From these samples, 231 core plugs were used for porosity measurement and 250 for permeability measurement. Additionally, 126 representative cast thin sections were prepared for the identification of lithology, pore types, sedimentary microfacies, and diagenetic modifications. All samples were taken from the platform-margin reef-shoal successions of the Changxing Formation and can adequately capture the heterogeneity and overall characteristics of the target reservoir in the study area.

While this study integrates core, thin-section, and logging data, uncertainties inevitably exist due to the inherent heterogeneity of carbonate reservoirs and the limited spatial coverage of core samples. To address these uncertainties, we employed a multi-scale calibration approach. The uncertainty in porosity and permeability interpretation was minimized by calibrating conventional logs against the 481 core-plug

measurements. Furthermore, the identification of sedimentary microfacies involves a degree of subjectivity; therefore, we cross-validated facies interpretations using FMI imaging logs to ensure the reliability of the sedimentary framework. A sensitivity analysis for fracture prediction indicates that structural curvature is the most sensitive parameter, followed by fault proximity.

3.2 Experimental and Analytical Techniques

To systematically characterize the reservoir properties and clarify the main controlling factors of reservoir development in the Changxing Formation of the Huanglongchang area, the following integrated technical methods were employed:

(1) *Core observation and petrographic thin-section analysis.* Systematic core description was carried out to record lithology, color, sedimentary structures, dissolution pores, vugs, and fractures. Microscopically, cast thin sections were examined to differentiate pore types such as dissolution pores, intergranular pores, and moldic pores, following the carbonate rock classification scheme and porosity nomenclature [16, 17].

(2) *Reservoir physical property measurement.* Porosity and permeability of core samples were measured using conventional core analysis instruments with helium porosimetry and gas permeametry to obtain reliable petrophysical parameters. Statistical analysis was performed to characterize the distribution of low-porosity and low-permeability reservoirs, with reference to analytical procedures for carbonate reservoir petrophysics [18]. Measurement uncertainty was evaluated based on instrument precision and replicate tests. The helium porosimeter has a measurement accuracy of ± 0.01 porosity units, with a relative error of $< 2\%$ for porosity values above 2%. The gas permeameter has an accuracy of ± 0.001 mD, with a relative error of $< 3\%$ for permeability above 0.1 mD. For logging interpretation, the uncertainty in effective reservoir thickness identification is estimated to be $\pm 5\%$–8%, mainly derived from the selection of porosity and resistivity cut-off values.

(3) *Well logging data processing and integrated interpretation.* Conventional logging curves were standardized to eliminate environmental effects. Gamma-ray (GR) logs were used to distinguish high-energy reef-shoal facies, and triple-porosity logs (density, neutron, and sonic) combined with resistivity logs were applied to identify effective reservoir intervals, following the principles of carbonate reservoir log interpretation [19, 20]. In addition, FMI imaging logging data were integrated to identify and quantitatively characterize the occurrence and distribution of fractures and dissolution vugs [21].

(4) *Sedimentary microfacies analysis.* By integrating core observations, thin-section identification, and logging responses, the sedimentary facies and microfacies of the Changxing Formation were classified following the carbonate rock classification scheme of Embry and Klovan [16]. Physical property parameters of different microfacies were statistically compared to reveal the control of sedimentary facies belts on reservoir quality, with petrophysical evaluation of each facies conducted with reference to carbonate reservoir petrophysics [18].

(5) *Structural setting and fracture characterization.* Based on structural mapping of the study area, the thickness of fracture-developed intervals was measured at different structural positions. The coupling relationships among structural highs, fold curvature, and fracture development were analyzed to clarify the controlling mechanisms of tectonic location and fractures on reservoir productivity and quality, following analytical methods for naturally fractured reservoirs [21].

4 Results

4.1 Reservoir Space

Through systematic macroscopic core observation and microscopic petrographic analysis of red-stained cast thin sections, the reservoir spaces of the Changxing Formation carbonates in the Huanglongchang Block are confirmed to comprise three main types of reservoir space: pores, vugs, and fractures. All these reservoir spaces were modified and produced by multi-stage differential dissolution and diagenetic processes [22]. Various pore types are developed in the study area and can be further divided into secondary types, including intercrystalline dissolution pores, matrix dissolution pores, intragranular dissolution pores, intergranular dissolution pores, moldic pores, intraclast dissolution pores, biocavity pores, and inter-reef framework pores (Figure 2).

Microscopic observation of red-stained cast thin sections from 4361.35 m in Well HL5 reveals abundant, irregular dissolution pores widely distributed within dolomite reservoirs (Figure 2(a)). The core interval 4386.29–4386.99 m in Well HL5 consists of peloidal dolomite, in which structural fractures and dissolution vugs are extensively developed

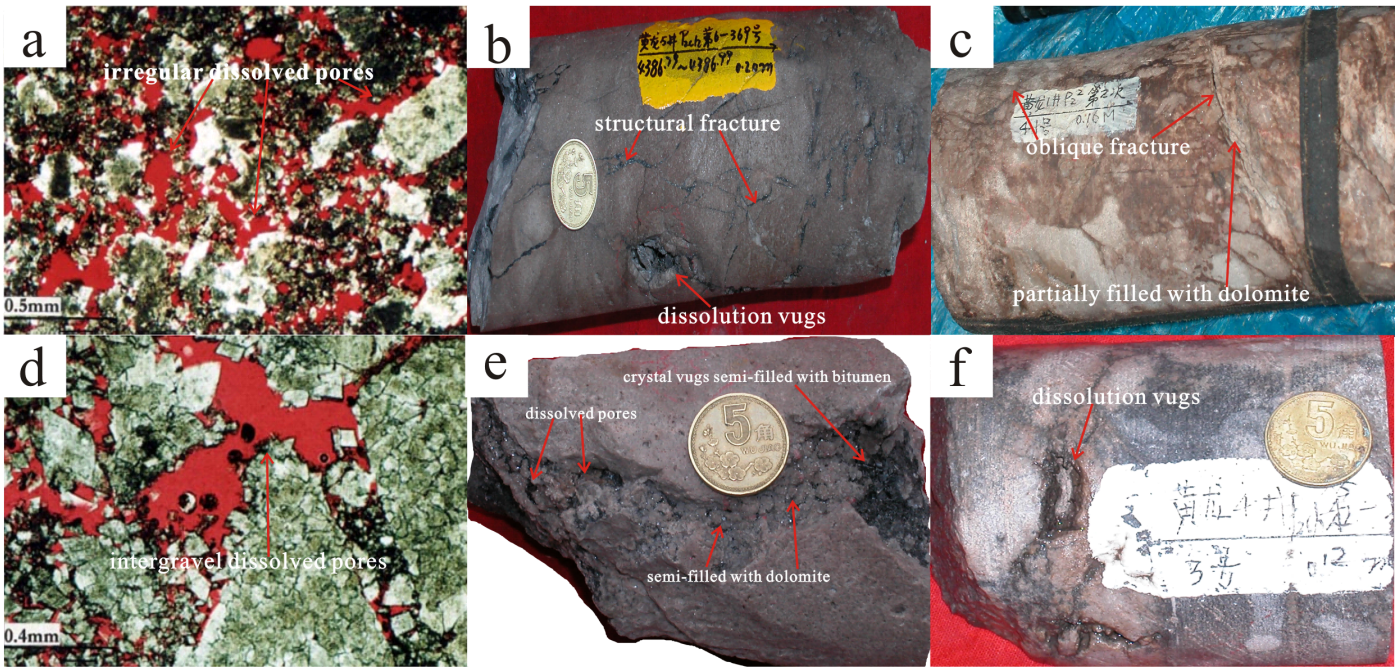


Figure 2. Core photographs and polarized-light photomicrographs of the Changxing Formation in HL wellfield. (a) A red cast thin-section photomicrograph shows well-developed irregular dissolved pores in dolomite, sample depth 4361.35 m. (b) Peloidal dolomite core developed with abundant fractures and dissolution vugs, sample depth 4386.29–4386.99 m. (c) Reef breccia dolomite develops oblique fractures partially filled with dolomite, sample depth 4241.12–4241.28 m. (d) A red cast thin section presents intense dissolution and developed intergranular/interclast dissolution pores in rudstone dolomite, sample depth 4232.21 m. (e) Dolomite core develops dissolved pores and crystal vugs semi-filled with dolomite and bitumen, sample depth 4376.31–4376.45 m. (f) Rudstone dolomite core characterized by widely developed dissolution vugs inside rocks, sample depth 4366.11–4366.23 m.

at the macroscopic scale (Figure 2(b)). Oblique fractures are pervasively developed in reef breccia dolomite at 4241.12–4241.28 m in Well HL1, with some fracture voids secondarily filled by dolomite minerals (Figure 2(c)). Thin-section samples from 4232.21 m in Well HL1 display well-developed intergranular dissolution pores in rudstone dolomite, indicating strong overall dissolution modification of the rock mass (Figure 2(d)). Dolomite cores from 4376.31–4376.45 m in Well HL5 contain not only common small dissolution pores but also large crystalline vugs semi-filled with dolomite and bitumen (Figure 2(e)). Under the influence of intense dissolution, rudstone dolomite at 4366.11–4366.23 m in Well HL4 is densely populated with dissolution vugs of various sizes, exhibiting excellent conditions for reservoir space development (Figure 2(f)).

4.2 Porosity and Permeability

Based on the measured porosity statistics of 231 core samples from the Changxing Formation reef reservoirs in the Huanglongchang area (Figure 3(a)), the porosity exhibits moderate dispersion with a pronounced centralized distribution. Porosity values are predominantly concentrated in the range of 4%–12%, with samples in this interval accounting for approximately 65% of the total. Samples with extremely low porosity ($< 4\%$) constitute the next most abundant group, making up about 23%. Samples with relatively high porosity ($> 12\%$) are the least common, representing only 12%. According to the porosity distribution pattern and industry evaluation standards, the Changxing Formation reef reservoirs are classified as low-porosity reservoirs.

Permeability measurements from 250 core samples (Figure 3(b)) indicate a wide range of values, reflecting strong reservoir heterogeneity. Samples with ultra-low permeability (< 0.1 mD) number 45, accounting for 18.00%. The dominant permeability range is 0.1–10 mD, containing the largest proportion with 127 samples (50.8%). A total of 73 samples fall within the moderate permeability range of 10–100 mD (29.2%), while only 5 samples (2%) exhibit high permeability (> 100 mD). Based on the reservoir property classification standard SY/T 6285-1997, the Changxing Formation reef reservoirs are generally characterized as low-permeability reservoirs. Overall, the studied reservoirs exhibit typical low-porosity and low-permeability properties with pronounced

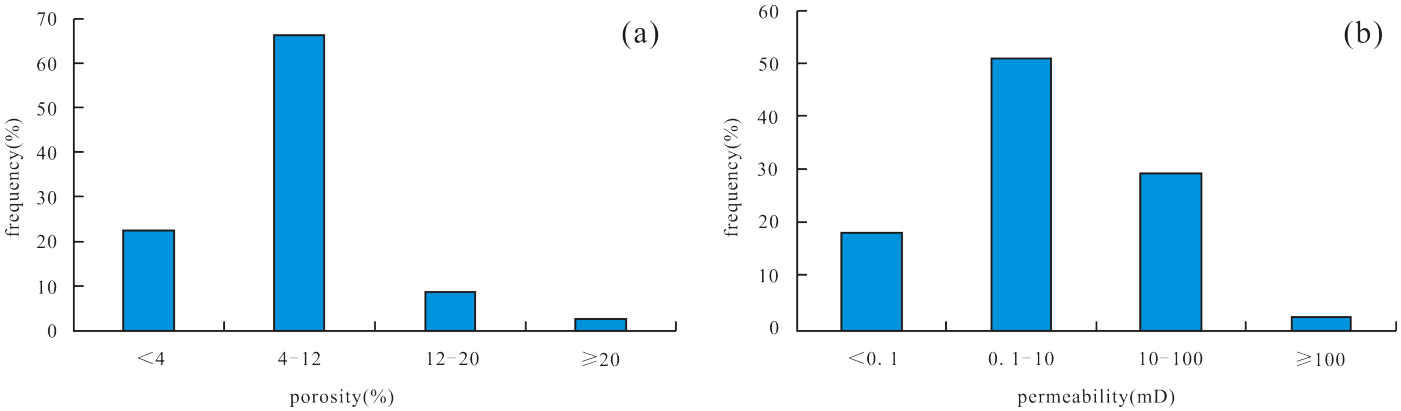


Figure 3. Histogram illustrating the statistical analysis of physical properties for core samples from the Changxing Formation in the Huanglongchang area. Panel (a) displays the distribution of the measured porosity values, while panel (b) shows the distribution of permeability values.

Table 1. Compositional distribution characteristics of natural gas in the Changxing Formation of the Huanglongchang area (gas composition in vol %).

Well	CH_4	C_2H_6	C_3H_8	n-C_4H_{10}	i-C_4H_{10}	CO_2	H_2S	N_2	H_2	He	Ar	Density	H_2S (g/m^3)	CO_2 (g/m^3)
HL1	96.38	0.16	0.01	0	0	2.46	0.33	0.63	0.03	0.029	0.009	0.583	5.034	48.235
HL2	97.41	0.27	0.01	0	0	1.77	0	0.49	0.015	0.021	0.002	0.574	0.008	34.706
HL4	96.03	0.17	0.01	0	0	2.42	0.85	0.46	0.038	0.028	0	0.585	12.106	47.451
HL5	92.86	0.1	0	0	0	1.97	4.54	0.46	0.047	0.024	0	0.604	64.947	38.705
HL8	95.85	0.15	0	0	0	2.68	0.82	0.48	0	0.024	0	0.5885	11.734	49.355
HL10	95.11	0.15	0	0	0	3.19	1.04	0.48	0	0.026	0	0.5948	14.872	58.747

heterogeneity, indicating moderate to poor reservoir quality.

4.3 Fluid in Gas Reservoir

Based on the natural gas analytical data from the Changxing Formation gas reservoirs in the Huanglongchang Structure (Table 1), methane is the predominant component, with its content ranging from 92.86% to 97.41%. Most wells exhibit methane content higher than 95%, displaying typical characteristics of thermogenic dry gas. Heavy hydrocarbon components are extremely low in abundance: ethane content is only 0.10%–0.27%, propane content generally does not exceed 0.01%, and neither n-butane nor isobutane is detected. The total heavy hydrocarbon content is less than 0.3%, reflecting the high maturity of the natural gas in this area.

With regard to non-hydrocarbon components, nitrogen content remains relatively stable at 0.46%–0.63%, and trace components such as hydrogen, helium, and argon are all present at ultra-low concentrations. Carbon dioxide and hydrogen sulfide are the main non-hydrocarbon gases, and their contents vary significantly among wells. Overall, the CO_2 content ranges from 1.77% to 3.19% by volume, corresponding to a mass concentration of 34.706–58.747 g/m^3, with relatively high CO_2 values observed in wells HL8 and HL10. The H_2S content varies from 0 to 4.54% by volume, with a corresponding mass concentration of 0–64.947 g/m^3. Among all tested wells, HL5 shows the highest H_2S content of 4.54%, whereas no H_2S is detected in HL2. These pronounced compositional differences reflect the fluid heterogeneity within the gas reservoirs and provide direct geochemical evidence for analyzing fluid-rock interactions and the reservoir modification history during hydrocarbon accumulation.

The relative density of the natural gas ranges from 0.574 to 0.604, being generally low, which is in good agreement with the dry-gas character dominated by high methane content. Due to its highest methane proportion and lowest non-hydrocarbon content, HL2 possesses the minimum relative density of 0.574. In contrast, influenced by its high H_2S concentration, HL5 has the maximum relative density of 0.604 in the study area.

Combined with the gas geochemical characteristics and a systematic compilation and analysis of formation water data (Table 2), the geochemical signatures of the Changxing Formation formation water also corroborate a favorable, strongly closed accumulation environment. The original formation water of the

Table 2. Distribution of water chemical analysis data for the Changxing Formation in the Huanglongchang Block (ion contents in mg/L; TDS in g/L).

Well	Na^+	K^+	Ca^{2+}	Mg^{2+}	Cl^-	SO_4^{2-}	HCO_3^-	I^-	Br^-	B	Water type	TDS
HL1	6855	175	1800	450	13974	966	1188	52	45	71	$CaCl_2$	25.54
HL4	9360	1542	40550	9200	115337	220	14	32	15	111	$CaCl_2$	177.26
HL8	7572	1930	39550	6875	103720	242	620	17	49	75	$CaCl_2$	161.16
HL10	2356	50	14715	7550	51563	159	178	4	10	< 1	$CaCl_2$	76.62

Changxing Formation is predominantly of the calcium chloride type. Cation composition is dominated by Ca^{2+} and Na^+; notably, the Ca^{2+} content in the original formation water of HL4 and HL8 is as high as 39,550–40,550 mg/L, exceeding the Na^+ content in the same intervals and constituting a distinctive geochemical signature of the formation water in this area. Mg^{2+} and K^+ are present in subordinate amounts. Anions are dominated by Cl^-, with contents ranging from 13,974 to 115,337 mg/L. SO_4^{2-} and HCO_3^- contents range from 75 to 966 mg/L and 14 to 1188 mg/L, respectively. Trace elements such as I, Br, and B are commonly detected in the formation water, with contents of 4–52 mg/L, 10–49 mg/L, and $<$ 1–111 mg/L, respectively, further indicating the geochemical environment for hydrocarbon migration and accumulation.

The original formation water of the Changxing Formation generally exhibits extremely high total dissolved solids (TDS), ranging from 25.54 to 177.26 g/L (14,900–177,260 mg/L), with an average value of approximately 110.15 g/L. In particular, the TDS of HL4 is as high as 177.26 g/L and that of HL8 reaches 161.16 g/L, both falling within the category of typical high-concentration brines. This specific ion assemblage and the extremely high TDS are products of long-term water-rock interaction and evaporative concentration, as well as typical indicators of a strongly closed accumulation environment, which is highly consistent with the closed accumulation setting indicated by the natural gas geochemical parameters.

The significant negative correlation between H_2S and CH_4 contents is a typical geochemical signature of thermochemical sulfate reduction (TSR). During TSR, sulfate minerals react with hydrocarbons at elevated temperatures, consuming methane and generating H_2S and CO_2. The higher H_2S content in HL5 indicates more intense TSR alteration in this well area, which is consistent with its greater burial depth and higher formation temperature. TSR not only modifies the gas composition but also produces acidic fluids that dissolve carbonate minerals and create secondary dissolution pores, serving as an important constructive diagenetic process for reservoir quality improvement.

The ultra-high TDS values (177.26 g/L in HL4 and 161.16 g/L in HL8) far exceed the average level of Changxing Formation formation water in northeastern Sichuan Basin (generally 50–100 g/L), indicating that these well areas are situated in a more strongly closed hydrodynamic environment with extremely limited water-rock exchange. This also implies that there may be a certain degree of compartmentalization within the gas reservoir: the HL4-HL8 area has better sealing conditions and more concentrated fluids, whereas HL1 and HL10 exhibit relatively lower TDS and slightly better connectivity. Such compartmentalization should be taken into consideration in reserve estimation and development plan design.

5 Discussion

5.1 Gas Reservoir Characteristics

5.1.1 Reservoir Characteristics

Based on systematic macroscopic and detailed core observations from the Huanglongchang Block, integrated with petrographic analysis of cast thin sections, comprehensive logging interpretation, and previous studies on the Changxing Formation reef reservoirs in the Sichuan Basin, the reservoir characteristics of the Huanglongchang Block are similar to those of other Changxing Formation reef reservoir areas in northeastern Sichuan Basin. They are classified as reef-shoal carbonate reservoirs and possess favorable conditions for forming large-scale natural gas accumulations. This study confirms that the Changxing Formation reservoirs in the Huanglongchang Block are mainly developed within reef facies belts, and the reservoir rocks are dominated by oolitic dolomite, reef breccia dolomite, and rudstone dolomite [23].

The reservoir space types are diverse, comprising

Table 3. Comparison of Changxing Formation reservoir characteristics among typical gas fields in northeastern Sichuan.

Gas field	Main lithology	Main pore type	Average porosity (%)	Average permeability (mD)	Main controlling factors
Puguang	Oolitic dolomite, reef dolomite	Intergranular dissolved pores, vugs	8–15	10–100	Sedimentary facies + supergene karst + burial dissolution
Luojiazhai	Reef dolomite, bioclastic dolomite	Intercrystalline dissolved pores, vugs	6–12	1–10	Platform margin reef + dolomitization + fractures
Huanglongchang	Oolitic dolomite, reef breccia dolomite	Intercrystalline dissolved pores, matrix dissolved pores	4–12	0.1–10	Back-reef shoal + multi-stage dolomitization + tectonic fractures
Yuanba	Crystalline dolomite, reef dolomite	Intercrystalline pores, dissolution vugs	3–8	0.01–1	Deep burial dolomitization + burial dissolution

pores, vugs, and fractures, but secondary porosity constitutes the primary reservoir porosity type. Specifically, secondary pores include intercrystalline dissolution pores, matrix dissolution pores, intragranular dissolution pores, intergranular dissolution pores, moldic pores, intraclast dissolution pores, biological cavity pores, and inter-reef framework pores (Figure 2). Intercrystalline dissolution pores, matrix dissolution pores, and intergranular dissolution pores are widely developed in the three aforementioned dolomite types, mostly exhibiting irregular shapes. Microscopic observation of cast thin sections at 4361.35 m in Well HL5 reveals that such irregular dissolution pores are extensively developed in dolomite reservoirs (Figure 2(a)). Intragranular dissolution pores, moldic pores, and intraclast dissolution pores occur primarily in oolitic dolomites, whereas biological cavity pores and inter-reef framework pores are concentrated in reef breccia dolomites and rudstone dolomites. Thin-section samples from 4232.21 m in Well HL1 demonstrate well-developed intergranular dissolution pores in rudstone dolomites, indicating intense dissolution modification of the entire rock mass (Figure 2(d)).

Abundant dissolution vugs are visible in cores, with dolomite and bitumen as the main fillings, mostly in a semi-filled state (Figure 2(e)). Under the influence of intense dissolution, dissolution vugs of varying sizes are densely developed in rudstone dolomites in the interval 4366.11–4366.23 m in Well HL4 (Figure 2(f)). In addition to the widespread occurrence of microscopic dissolution pores, large vugs are also present in the interval 4376.31–4376.45 m in Well HL5. Fractures are dominated by structural fractures, among which oblique fractures are extremely well developed, and some fracture voids are subsequently filled by dolomite minerals (Figure 2(c)). In the oolitic dolomites of the interval 4386.29–4386.99 m in Well HL5, the macro-scale coexistence of extensively developed structural fractures and dissolution vugs can be observed (Figure 2(b)).

Based on measured porosity statistics from 231 core samples of the Changxing Formation reef reservoirs in the Huanglongchang area (Figure 3(a)), porosity exhibits moderate dispersion and a pronounced centralized distribution. Porosity values are mainly concentrated in the range of 4%–12%, with samples in this interval accounting for approximately 65% of the total; ultra-low porosity samples ($< 4\%$) account for about 23%; relatively high porosity samples ($> 12\%$) are the least, representing only 12%. Permeability data from 250 core samples (Figure 3(b)) reveal wide variability, reflecting strong reservoir heterogeneity. Forty-five samples fall into the ultra-low permeability category (< 0.1 mD), accounting for 18.00%; the dominant permeability range is 0.1–10 mD, containing 127 samples (50.80%); 73 samples have moderate permeability (10–100 mD, 29.20%); and only 5 samples (2.00%) exhibit high permeability (> 100 mD). With reference to industry standards, the Changxing Formation reef reservoirs in the Huanglongchang Block are generally classified as low-porosity and low-permeability reservoirs with prominent heterogeneity and moderate overall reservoir quality. However, relatively high-permeability intervals can locally form due to enhanced fracture-pore connectivity.

Compared with typical Changxing Formation gas fields in northeastern Sichuan Basin (Table 3), the Huanglongchang reservoir shares similar lithology and pore types with the Puguang and Luojiazhai gas fields, all being dominated by dolomite and secondary dissolution pores. Nevertheless, the overall porosity and permeability of the Huanglongchang reservoir are slightly lower, primarily due to relatively weaker karstification intensity and thinner reef-shoal body thickness. In terms of fracture development,

Huanglongchang ranks at an intermediate level among the gas fields in the steep structural belt, weaker than the strongly deformed Qilixia Structure but stronger than areas with gentle structural deformation.

5.1.2 Gas Reservoir Fluid Characteristics

Original formation pressure and temperature data for the Changxing Formation gas reservoir in the Huanglongchang Structure are presented in Table 4. The formation pressure ranges from 42.55 to 46.25 MPa. When converted to a common datum, the formation pressures fall between 42.60 and 44.95 MPa, corresponding to pressure coefficients of 1.081–1.202. The formation temperature ranges from 94.14 to 101.14 °C. Using a commonly accepted surface temperature of 15 °C for oil and gas reservoirs, the geothermal gradient is calculated to be 1.97–2.19 °C/100 m. These parameters indicate that the gas reservoir belongs to a normal-pressure to slightly overpressured system under a normal geothermal gradient. The geochemical characteristics of the gas are further consistent with regional studies that attribute the principal gas source around the Kaijiang-Liangping Trough to the Upper Permian Longtan Formation, with varying contributions from thermogenic cracking gas [25]. The converted formation pressures and mid-reservoir temperatures show only minor differences among wells HL1, HL4, and HL5, reflecting similar temperature–pressure conditions. This consistency demonstrates comparable accumulation conditions across different well blocks and confirms that they belong to the same gas reservoir system.

Table 4. Measured formation pressure and temperature values for the Changxing Formation gas reservoir in the Huanglongchang Structure.

Parameter	HL1	HL4	HL5
Vertical depth at the middle of the production layer (m)	4003.5	3613	4365
Formation pressure (MPa)	42.599	42.548	46.249
Pressure coefficient	1.086	1.202	1.081
Temperature at the middle of the production layer (°C)	96.02	94.14	101.14

The natural gas in the Changxing Formation gas reservoir of the Huanglongchang Structure has a dryness coefficient greater than 0.99 and is dominated by dry gas. Compositional analysis shows that methane is the principal component, with contents ranging from 92.86% to 97.41%; most wells exhibit methane contents above 95%. Heavy hydrocarbon components are extremely low: ethane content is 0.10%–0.27%, propane content generally does not exceed 0.01%, and neither n-butane nor isobutane is detected. The total heavy hydrocarbon content is less than 0.3%, indicating high thermal maturity. Among the non-hydrocarbon components, nitrogen content is stable at 0.46%–0.63%, while trace components such as hydrogen, helium, and argon occur at ultra-low levels. Carbon dioxide and hydrogen sulfide are the main non-hydrocarbon gases, with pronounced inter-well variations: CO_2 content by volume is 1.77%–3.19%, corresponding to mass concentrations of 34.706–58.747 g/m^3, with relatively higher values in wells HL8 and HL10. H_2S content ranges from 0 to 4.54% by volume, corresponding to mass concentrations of 0–64.947 g/m^3. Well HL5 has the highest H_2S content (4.54%), whereas no H_2S is detected in well HL2. This marked compositional difference reflects fluid heterogeneity within the gas reservoir. The relative density of the natural gas ranges from 0.574 to 0.604, which is generally low and consistent with the dry-gas character dominated by methane. Well HL2 has the lowest relative density owing to the highest methane proportion and the lowest non-hydrocarbon content, while well HL5 has the highest relative density in the area due to its elevated H_2S content.

Formation water analyses show that K^+ concentrations range from 50–1930 mg/L, Na^+ from 2356 to 9360 mg/L, Ca^{2+} from 1800 to 40,550 mg/L, Mg^{2+} from 450 to 9200 mg/L, Cl^- from 13,974 to 115,337 mg/L, and SO_4^{2-} from 159 to 966 mg/L. The total dissolved solids (TDS) of the formation water range from 14,900 to 177,260 mg/L.

5.2 Gas Reservoir Control Factors

5.2.1 Sedimentary Environment

The sedimentary environment is the primary geological factor controlling the formation and distribution of the Changxingian reef gas reservoirs in the Huanglongchang area. It not only determines the original material basis and spatial distribution pattern of the reservoirs, but also profoundly influences the types and intensity of subsequent diagenesis as well as the favorable sites for hydrocarbon migration and accumulation.

The Kaijiang-Liangping Trough formed during the early Early Triassic and presents an overall asymmetric, half-graben-like faulted trough extending in a northeast direction, with a steep southwestern flank and a gentle northeastern flank. Its evolution can be traced back to the early stage of the Upper

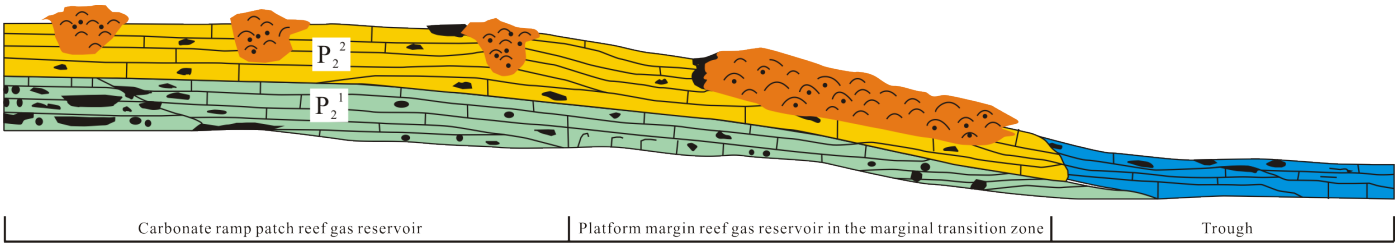


Figure 4. Sedimentary model of the Changxing Formation, Huanglongchang Block.

Permian deposition, when a carbonate ramp geomorphology continuously dipping toward the northeast had already developed in the eastern Sichuan Basin. The Huanglongchang Structure is precisely located at the critical transition from this ramp to the Kaijiang-Liangping Trough, sitting within a three-level sedimentary geomorphic transition zone of trough–platform margin–deep ramp during the Changxingian (Figure 4). This unique paleogeographic position created exceptional conditions for the development of platform-margin reefs [6, 7].

Through systematic core observation, analysis of well logging response characteristics, and integration with previous studies on the sedimentary framework of the Changxing Formation in eastern Sichuan, this study concludes that the platform-margin facies is the sedimentary facies belt with the greatest exploration potential in the Changxing Formation of the Huanglongchang area. This facies belt is distributed in a zonal pattern around the trough, forming a transitional geomorphic unit between the deep ramp and the trough basin. The sedimentary setting is a deep-water slope environment with water depths ranging from tens to more than one hundred meters, and its most prominent feature is the development of large-scale platform-margin reefs. Compared with the small, isolated patch reefs within the ramp, platform-margin reefs are discontinuously distributed along the platform margin in a beaded pattern, with larger individual reef bodies, better lateral continuity, and more complex reef assemblages. These reef-shoal complexes comprise several sedimentary microfacies, principally including reef core, back-reef shoal, fore-reef shoal, and fore-reef ramp. The vast majority of these reef bodies have ultimately been transformed into high-quality dolomitic reservoir bodies, which have become the main sites for hydrocarbon accumulation. The Changxingian biogenic reefs developed in the Huanglongchang Structure belong to typical platform-margin reefs, with their reservoirs mainly developed in the middle to upper part of the Changxing Formation (Member 2 to Member 3). These reef bodies exhibit extensive distribution and thick reef complexes, providing the material basis for the formation of medium- to large-scale hydrocarbon reservoirs.

Sediments formed under different depositional environments show significant differences in mineral composition, grain fabric, grain-size distribution, sorting and roundness, single-layer thickness, and sedimentary structures. These differences directly determine the degree of original porosity development and the potential for subsequent diagenetic modification. Sedimentary facies belts with favorable original reservoir properties are more conducive to preserving and improving reservoir quality during later diagenetic evolution, ultimately forming high-quality reservoir zones. Even within the same sedimentary facies belt, the reservoir properties of different microfacies often display pronounced heterogeneity. To quantitatively characterize the reservoir quality differences among the sedimentary microfacies of the Changxing Formation in the Huanglongchang area, this study conducted systematic porosity measurements on 77 core samples. The results show that the average porosity of the back-reef shoal microfacies (33 samples, 43% of the total) is 4.72%, whereas the average porosities of the reef-core and fore-reef slope microfacies are only 1.36% and 1.28%, respectively. Further analysis of 26 effective reservoir samples with porosity greater than 3% reveals that the back-reef shoal microfacies accounts for 62% (16 samples) of the effective samples, with an average porosity as high as 8.75%; the reef-core microfacies accounts for 31% (8 samples), with an average porosity of 4.60%; and the fore-reef slope microfacies accounts for only 7% (2 samples), with an average porosity of 5.23%.

The above data clearly indicate that the back-reef shoal microfacies exhibits the best reservoir properties in the Changxing Formation of the Huanglongchang area. This is primarily attributed to its relatively

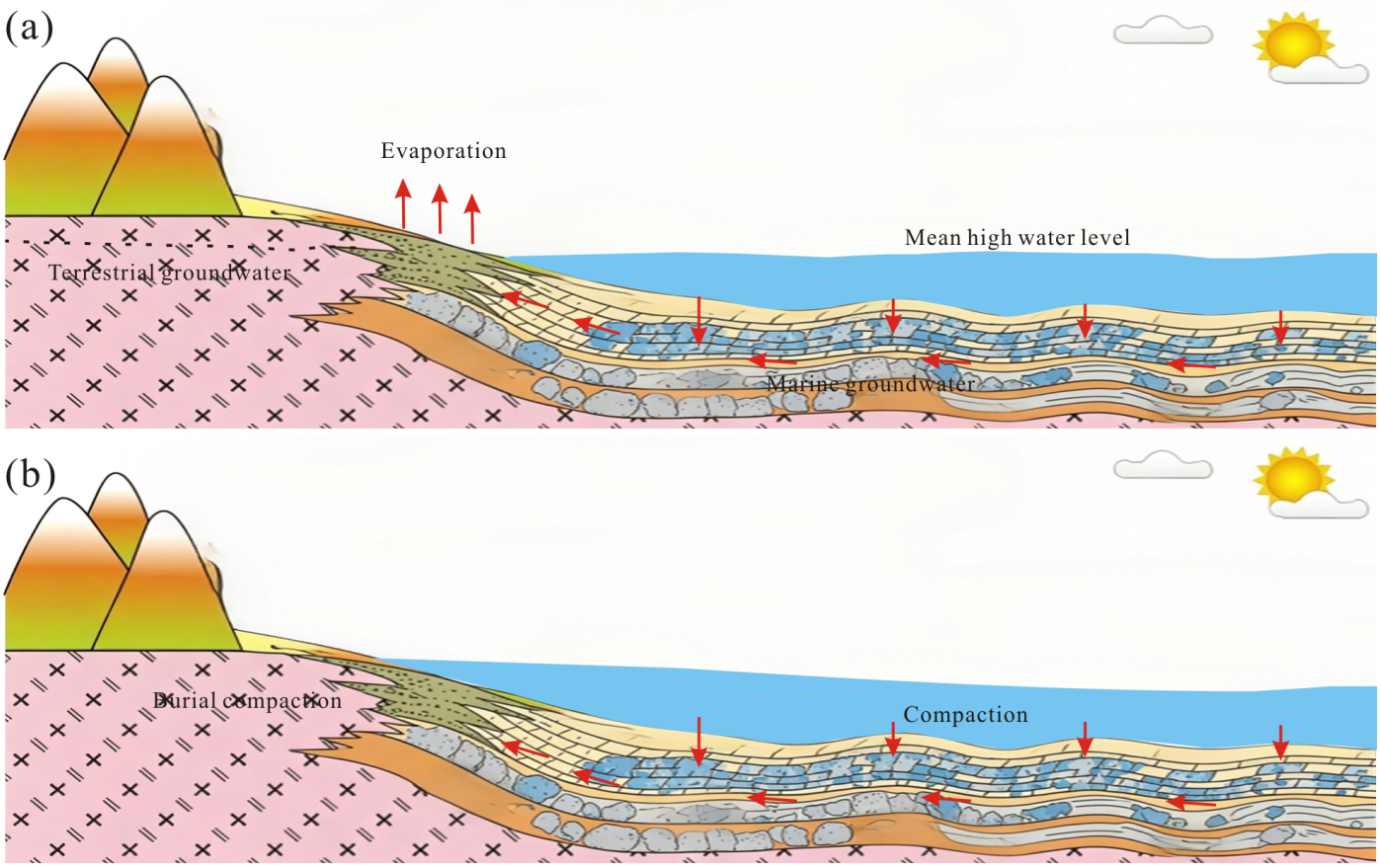


Figure 5. Genetic model of dolomitization for the Changxing Formation in the Huanglongchang area. (a) Evaporative pumping dolomitization model; (b) Burial dolomitization model.

high-energy, turbulent-water depositional setting, where sediments are dominated by sparry grainstone with good sorting and roundness and well-developed primary intergranular pores. These characteristics provide excellent fluid pathways and reaction space for subsequent dolomitization and dissolution. In contrast, the reef core consists mainly of bindstone and framestone, in which primary pores are relatively well developed but easily occluded by cements during early diagenesis. The fore-reef slope is dominated by brecciated limestone and micritic limestone deposited by gravity flows, with extremely low primary porosity. This understanding provides an important geological basis for refined exploration and favorable target optimization of the Changxingian reef gas reservoirs in the Huanglongchang area.

5.2.2 Diagenesis

Based on detailed petrographic observations and systematic analysis of dolomitizing fluid properties, the dolomites of the Changxing Formation in the Huanglongchang area can be classified into multiple genetic types, whose formation and evolution are closely linked to fluid activities and tectonic settings. Micritic dolomite is characterized by a tight lithology, scarce bioclasts, and extremely poorly developed primary pores, indicating formation under a strongly evaporative environment with restricted water circulation (Figure 5(a)). Persistent evaporative concentration during the Late Permian generated high-salinity marine brines that supplied abundant Mg^{2+} for dolomitization, and penecontemporaneous micro- to finely crystalline dolomite was produced via evaporative pumping under near-surface conditions.

The burial diagenetic stage represents the critical interval for dolomite generation in the study area, during which both residual reef-textured dolomite and crystalline dolomite were formed. Their typical petrographic signature is the selective dolomitization of grain components and reef-building biotic frameworks (Figure 5(b)) [24]. The dolomitizing fluids were predominantly high-salinity recycled marine pore waters derived from the dissolution of Early-Middle Triassic evaporites. These fluids migrated along pre-existing faults, fracture networks, and stratigraphic discontinuities, preferentially altering carbonate rocks within the reef-core, back-reef-shoal, and fore-reef-shoal microfacies of

Table 5. Diagenetic evolution sequence and pore evolution of Changxing Formation reservoirs.

Diagenetic stage	Geological period	Major diagenetic events	Effect on reservoir quality	Porosity evolution
Syndepositional stage	Late Permian Changxingian	Marine cementation, evaporative pumping dolomitization, syndepositional karst	Early cementation reduces primary pores; dolomitization preserves pore framework; syndepositional dissolution increases porosity	Initial porosity ~30%–40%, decreases to ~20%–25% after early cementation
Eodiagenesis stage	Late Permian–Early Triassic	Shallow burial compaction, pressure solution, early burial dolomitization	Compaction destroys primary pores; burial dolomitization forms intercrystalline pores and resists further compaction	Porosity decreases to ~10%–15%
Mesodiagenesis stage	Triassic–Cretaceous	Medium-deep burial dolomitization, organic acid dissolution, TSR dissolution	Multi-stage dolomitization continues; organic acids and TSR fluids form a large number of secondary dissolution pores	Porosity first decreases then increases, maintained at 4%–12%
Telodiagenesis stage	Late Cretaceous–Quaternary	Tectonic fracturing, late cementation, bitumen filling	Tectonic fractures significantly improve permeability; late filling partially reduces pores and throats	Final reservoir formation, fracture-vug-pore composite reservoir space

the platform-margin reef-shoal system. Multi-stage superimposed burial dolomitization occurred throughout the early, middle, and late diagenetic periods. During the late diagenetic stage, intense tectonic perturbations induced by the Yanshanian and Himalayan orogenies triggered structural fracturing of the dolomite reservoirs, producing tectonic cataclastic dolomite.

The formation and distribution of the Changxing Formation gas reservoirs in the Huanglongchang area are fundamentally governed by the integrated diagenetic evolutionary sequence, exhibiting a diagenesis-controlled reservoir model summarized as: sedimentary facies lay the foundational framework, constructive diagenesis expands reservoir storage capacity, fracture systems boost gas productivity, and effective preservation conditions provide the ultimate trapping safeguard. Specifically, the high-energy platform-margin reef-shoal facies establish the primary pore network for reservoir development; burial dolomitization fueled by high-salinity marine pore waters derived from the dissolution of Early-Middle Triassic evaporites not only forms a rigid intercrystalline pore framework with strong compaction resistance, but also effectively prevents pore collapse during deep burial; superimposed modification by early supergene dissolution, burial organic-acid dissolution, and thermochemical sulfate reduction (TSR) dissolution substantially enlarges the effective reservoir pore volume; and fracture networks generated by tectonic fracturing serve as critical seepage pathways sustaining high gas-well deliverability.

Based on petrographic cross-cutting relationships, burial history, and tectonic evolution, the diagenetic evolution of the Changxing Formation reservoir can be divided into four stages, as summarized in Table 5.

Calcite cementation and chemical compaction (pressure solution) constitute the primary destructive processes responsible for porosity reduction in the reservoirs. The long-term preservation of gas accumulations depends on two critical factors: first, an overpressured compartment confined by the tight strata of the Wujiaping Formation and the first member of the Feixianguan Formation, which strongly inhibits pressure dissolution; second, the intensity of tectonic deformation, which controls cap-rock integrity. Together, these two factors ensure effective gas retention under deep burial conditions.

5.2.3 Tectonism

The multi-stage tectonic movements spanning the Yanshanian to Himalayan periods imposed superimposed modification on the stress field of the Changxing Formation in the Huanglongchang area, ultimately generating multi-stage fracture systems with pronounced differences in development intensity, fracture types, and reservoir effectiveness across structural positions.

The first-stage failure-degree zoning map of the Changxing Formation (Figure 6(a)) reveals the initial fracture pattern under early tectonic deformation. Fractures of this stage are dominated by planar conjugate X-shaped shear fractures, displaying an overall directional and organized distribution. The second-stage failure-degree zoning map (Figure 6(b)) reflects the final failure characteristics after late-stage tectonic superimposition. With the widespread development of high-angle tensile fractures and derived fractures, the connectivity of the fracture

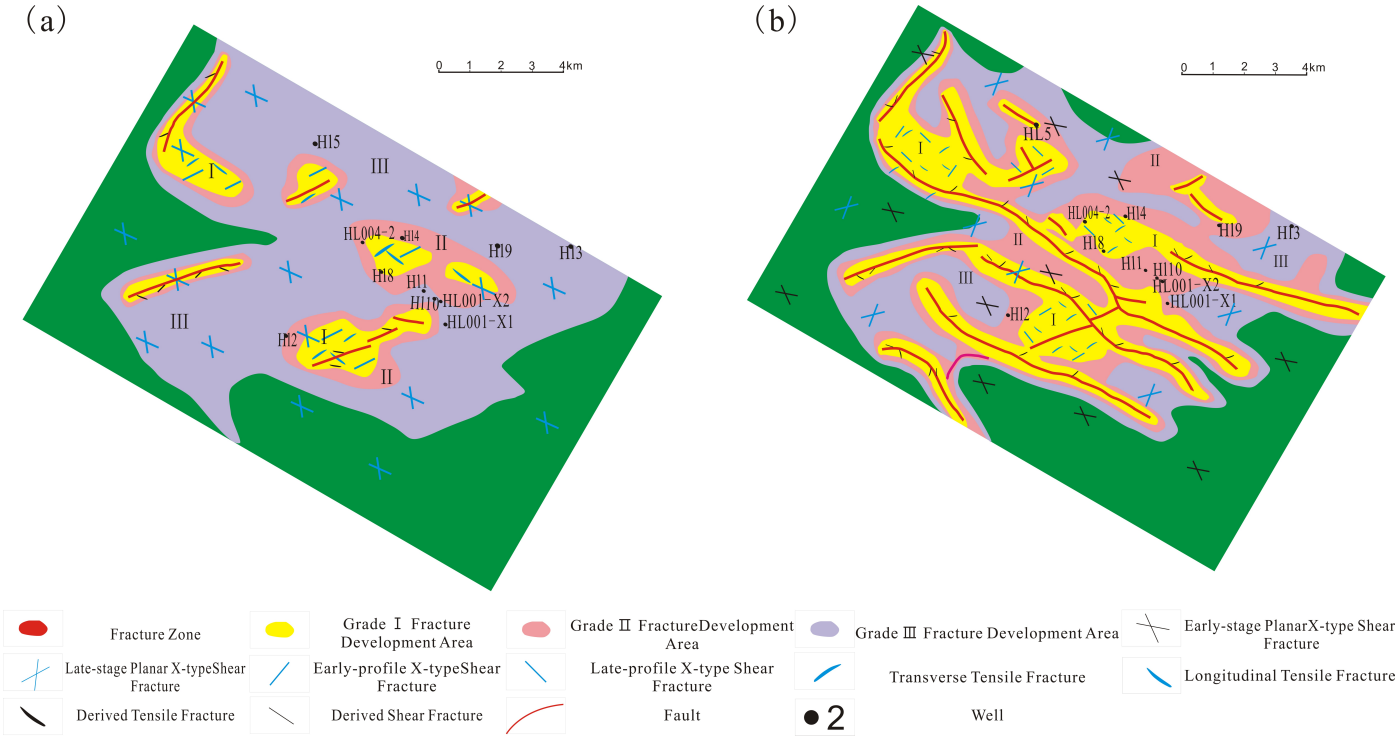


Figure 6. Rock failure degree zonation map of the Changxing Formation in Huanglong field for different stages. (a) Stage I; (b) Stage II.

network is substantially enhanced, and the reservoir effectiveness is significantly improved compared with the early stage.

Further characterization based on the two-stage zoning results indicates that the fault zone at the top of the Changxing Formation in the Huanglongchang Structure extends generally along the strike of the main fault, and its formation and evolution are strictly controlled by the transition between the two stages of tectonic stress fields. The NW–SE trending faults in the study area formed during the early tectonic stage, when the stress intensity was relatively weak and the resulting faults were generally small in scale, corresponding to a rock-mass failure degree greater than 1.45 within the fault zone. In the late tectonic stage, the principal stress direction shifted from SE to NE, accompanied by a marked increase in stress intensity. This not only generated larger-scale NE-trending faults but also produced large-scale fold structures, further raising the rock-mass failure degree in the fault zone to above 1.50. The genetic types of fractures in the area are consistent with those at the bottom of Member 4 of the Feixianguan Formation, dominated by fault-associated high- and low-angle shear fractures and tensile fractures, with dominant strikes in the NW and NE directions.

(1) *Class I Fracture Development Zone.* The Class I fracture development zone represents the core zone with the most intensive fracturing. It is concentrated at structural highs, on both flanks of faults, at fault tips, and at fault inflection points and intersections within the study area. From the perspective of staged evolution, the early Class I zone was distributed in a NE–SW direction along the fault zone; in the late stage, with the deflection of the principal stress direction, the development zone reoriented to a NW-SE direction along the faults. The rock-mass failure degree in the late stage is overall higher than that in the early stage: the early-stage value ranges from 1.300 to 1.450, while the late-stage value rises to 1.363–1.500; such failure-degree classification follows the finite-element paleostress simulation approach established for ultradeep marine carbonate reservoirs in the Sichuan Basin [26]. Fractures in this zone are dominated by high-angle shear fractures and high-angle tensile fractures formed in the early stage, with dominant strikes including nearly NW, nearly E-W, and nearly N-S directions, characterized by high fracture density and favorable connectivity.

(2) *Class II Fracture Development Zone.* The Class II fracture development zone is mainly distributed around the periphery of the Class I zone and around secondary faults in the area. It generally forms a NW-trending annular belt surrounding the Class I fracture zone and is concentrated on the peripheral

Table 6. Correspondence relationship between structural positions and fracture development intervals in the Huanglongchang Block.

Well name	Structure position	Thickness of fracture development (m)
HL1	Huanglongchang structural high	20.20
HL2	High position of the western structural high, Huanglongchang Structure	23.44
HL3	Northern flank of the nose structure at the eastern end of the main structural high, Huanglongchang Structure	2.04
HL5	Fujiapo structural high	26.54
HL005-c1	Periphery of the Fujiapo structural high, Huanglongchang Structure	7.12
HL8	Axial part of the main structural high, Huanglongchang Structure	14.94
HL9	Axial part at the eastern end of the main structural high, Huanglongchang Structure	9.18
HL10	Eastern axis of the main structural high, Huanglongchang Structure	35.20

slopes of each structural high of the Huanglongchang Structure. This zone is primarily controlled by the late tectonic stress field, with weak overprinting from early tectonic processes. Driven by the large stress difference in the late stage, the rock-mass failure degree in the late stage is significantly higher than that in the early stage. The first-stage failure degree at the top of the Changxing Formation is 1.168–1.300, and the second-stage value is 1.170–1.363. Comprehensive evaluation indicates that fractures are relatively well developed in this zone, comprising high-angle and low-angle shear fractures as well as tensile fractures, and forming an integrated fracture system with multiple coexisting sets of nearly E-W, nearly N-S, NE, and NW strikes.

(3) *Class III Fracture Development Zone.* The Class III fracture development zone is the area with the weakest fracture intensity in the study area. It is mainly distributed beyond the Class I and Class II zones of the Huanglongchang structural high, West Huanglongchang buried structural high, Fujiapo buried structural high, and West Fujiapo buried structural high, as well as in the intervals between Fault Huang (1) and Huang (2), between Fault Huang (2) and Huang (3), and the area northeast of Fault Huang (4). This zone is also dominated by the late tectonic stress field, with extremely limited influence from early tectonic activities. The extension direction of the fracture development zone is broadly consistent with the strike of regional main faults, showing an overall NW distribution. The first-stage rock-mass failure degree at the top of the Changxing Formation ranges from 1.070 to 1.168, and the second-stage value ranges from 1.080 to 1.170.

With respect to fracture effectiveness, the three fracture development classes exhibit distinct differences in connectivity and permeability characteristics. Sensitivity analysis shows that fracture development degree is most sensitive to fold curvature: when curvature increases by 0.1 km^{-1}, the rock-mass failure degree increases by approximately 0.06 on average. Structural position is the second most sensitive factor, with a difference of about 0.2–0.3 in failure degree between structural highs and limbs. Fracture connectivity directly determines the seepage capacity of the reservoir. Class I fracture zones are dominated by interconnected network fractures, with connectivity coefficients greater than 0.7, forming high-permeability channels; in these zones, effective permeability can be 1–2 orders of magnitude higher than matrix permeability, and gas wells generally exhibit high and stable production. Class II fracture zones have moderate connectivity, with coexisting isolated fractures and local network fractures and connectivity coefficients of 0.3–0.7, corresponding to medium productivity. Class III zones are characterized by poor connectivity with mostly isolated fractures, and fractures contribute little to the overall permeability. The strong anisotropy of fracture networks also leads to significant directional differences in fluid flow: permeability along the dominant fracture strike is 3–8 times higher than that perpendicular to the strike, which should be fully considered in well-pattern deployment and horizontal-well trajectory design.

Overall, the fracture development degree in the Class III zone is moderate, dominated by high-angle and low-angle shear fractures formed during the two stages of tectonic movements, with tensile fractures rarely developed. Both the storage capacity and seepage capacity of this zone are inferior to those of the Class I and Class II development zones.

Fold cores and zones of high structural curvature are dominated by high-angle tensile fractures and shear fractures with high density and good connectivity, and are classified as high fracture-development sections in both stages of the zoning maps. Network fractures and interbreccia pores are widely developed in fault zones and their damage zones, acting as the main pathways for fluid migration in the area and corresponding to the core fracture zones in the zoning maps. In the weathering and leaching zone beneath the Permian-Triassic (P-T) unconformity, tectonic fractures and supergene dissolution vugs are superimposed, forming a fracture-vug integrated reservoir architecture that further improves the reservoir performance of fracture development zones [27]. The superimposed area of platform-margin reef-shoal bodies and structural highs is governed by both sedimentary heterogeneity and an extensional stress regime, exhibiting the most favorable fracture development degree and reservoir effectiveness. This area represents the most favorable reservoir zone with the highest comprehensive fracture development grade in the two-stage failure-degree zoning.

The disparities in fracture development and multi-stage evolution patterns across different structural positions directly control the spatial distribution of reservoir quality in the Changxing Formation (Table 6).

The coupled reservoir-controlling model of "sedimentary facies constraint, diagenetic modification, and tectonic fracture enhancement" established in this study is generally applicable to platform-margin reef-shoal reservoirs along the Kaijiang-Liangping Trough, such as the Puguang, Yuanba, and Luojiazhai gas fields. The core concept—that the platform margin provides the material basis, multi-stage dolomitization and dissolution preserve and expand pore space, and tectonic fractures improve permeability—is universal for deeply buried reef-shoal carbonate reservoirs.

However, the relative contributions and dominant diagenetic processes may vary under different tectonic settings. For intra-platform patch reefs subjected to weak tectonic deformation, sedimentary facies and early diagenesis play a more dominant role, while the contribution of tectonic fractures diminishes significantly. In strongly deformed fold belts, tectonic fracturing may become the primary control on well productivity. This model can also serve as a reference for other Permian-Triassic reef-shoal reservoirs in the Tethyan realm, although it needs to be calibrated against local diagenetic and tectonic evolution histories.

5.2.4 *Reservoir Conditions*

High-quality reservoirs in the Changxing Formation platform margin of the Huanglongchang area are jointly controlled by sedimentary facies and multi-stage karstification, with gas pay zones primarily developed within reef-shoal complexes.

During the early Changxing Formation, gentle paleotopography and continuous transgression produced open, low-hydrodynamic water bodies. Lithologies are dominated by low-energy micrite, muddy micrite and argillaceous limestone, corresponding to open platform and lower platform margin slope microfacies. Only on local inherited paleohighs did reef-building organisms (sponges, hydrozoans, bryozoans, etc.) thrive under clear water, sufficient light and abundant nutrients, forming small patch reefs and shoals. These reef-shoal bodies are small in scale with poor reservoir quality: they are laterally isolated by tight micrite and argillaceous limestone, and vertically stacked as thin beds.

During the middle-late Changxing Formation, rapid relative regression caused progressive shallowing of sedimentary water and significantly enhanced hydrodynamics. Favorable sunlight and salinity conditions promoted massive proliferation of reef-building and reef-associated organisms. Deposits are dominated by reef framework limestone, bioclastic limestone and calcarenite (Figure 2), which constitute the main reservoir lithologies. Widely developed, laterally connected platform margin reef-shoal bodies replaced most low-energy micrite deposits, reducing inter-body compartmentalization and forming large-scale interconnected reef-shoal complexes with prominent multi-stage vertical stacking. These complexes contain abundant primary framework pores and intergranular pores; although partially filled by early diagenetic calcite cements, they still form relatively high-porosity and high-permeability intervals. These high-quality sedimentary facies belts provided favorable pathways for subsequent diagenetic fluids and laid the material foundation for secondary dissolution pore development, promoting later constructive diagenesis and prerequisites for widespread high-quality reservoirs in the study area.

During the late Changxing Formation, frequent sea-level fluctuations caused repeated subaerial exposure of platform margin reef-shoal bodies,

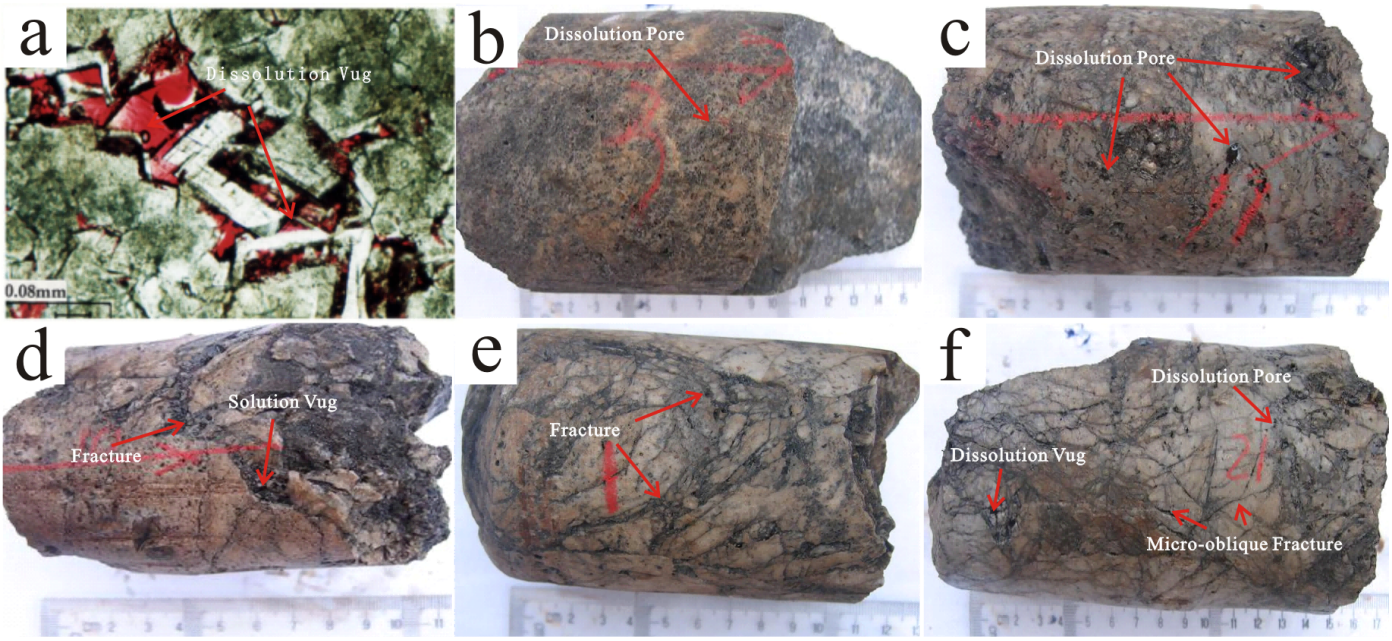


Figure 7. Microscopic photographs and hand specimen & core characteristics of syndepositional–supergene karst in the Changxing Formation, Huanglongchang area. (a) Microphotograph of rudstone dolomite with moldic pores; Well HL1, sampling depth 3957.6 m. (b) Dark gray finely crystalline vuggy dolomite with abundant dissolution pores and vugs; Well HL004-2, sampling depth 3490.05–3490.13 m. (c) Gray finely crystalline vuggy dolomite with well-developed but unevenly distributed dissolution pores and vugs; the plane porosity generally ranges from 1% to 3%, locally up to 3%–5%. A total of 262 small vugs, 92 medium vugs and 12 large vugs are identified, with euhedral calcite crystals observed on the wall of individual vugs; Well HL004-2, sampling depth 3490.93–3491.03 m. (d) Micritic dolomite with well-developed vugs and dissolution pores, as well as effective fractures and microfractures that mutually intersect; Well HL4, sampling depth 3509.89–3509.99 m. (e) Dark gray finely crystalline vuggy dolomite developed with horizontal and oblique microfractures; these fractures intersect to form a reticular network, and most pores, fractures and vugs are interconnected; Well HL5, sampling depth 4332.8–4332.93 m. (f) Light brownish-gray finely crystalline vuggy dolomite with abundant oblique microfractures intersecting small effective oblique and vertical fractures to form a reticular network; most pores, fractures and vugs are interconnected, and gas bleeding is detected at 42 pore-fracture points; Well HL8, sampling depth 3551.23–3551.33 m.

generating widespread syndepositional karstification (Figure 7(a-c)). This karstification corresponds to high-frequency reef-shoal sedimentary cycles and shows distinct cyclic layering. Meteoric freshwater leaching produced abundant selective dissolution pores (intragranular pores, moldic pores, framework dissolution pores, etc.), significantly expanding primary pore space and laying the groundwork for subsequent supergene karstification and burial dissolution. However, syndepositional karstification mainly occurs at the top of each sedimentary cycle, with thin single layers and multi-stage stacking. Partial dissolution pores were modified by early calcite cementation, limiting its independent contribution to reservoir quality improvement.

During the late Changxingian, relative sea-level fall and episodic subaerial exposure of the platform-margin reef-shoal bodies promoted meteoric-water leaching and supergene karstification. Prolonged exposure and meteoric dissolution enlarged pre-existing syndepositional pores and vugs and generated abundant non-fabric-selective dissolution pores, vugs, and dissolution fractures. These secondary dissolution spaces were subsequently modified and locally connected by burial dissolution and tectonic fracturing, resulting in a composite pore-vug-fracture reservoir system. The enhanced connectivity among pores, vugs, and fractures substantially improved reservoir storage and seepage capacity, thereby providing favorable storage space and migration pathways for natural gas (Figure 7(d-f)).

During burial diagenesis, organic acids and thermal evolution fluids derived from mature source rocks of the underlying Longtan Formation migrated into reef-shoal reservoirs. Syndepositional deformation structures within carbonate platforms, such as early-formed fractures and fault networks, serve as long-lived conduits for such diagenetic fluids [28]. The architecture of platform reef-shoal reservoir

bodies also controls the spatial heterogeneity of fluid migration pathways and dissolution intensity [29]. These fluids dissolved early cements and unstable minerals to form abundant secondary dissolution pores, further enhancing reservoir porosity and permeability. This process acts as a critical supplementary factor for high-quality reservoir formation in the study area.

In summary, high-quality gas reservoirs in the Changxing Formation platform margin of the Huanglongchang area result from the superimposed modification of sedimentary facies control and multi-stage karstification. Platform margin reef-shoal deposition provides the material basis for reservoir development; syndepositional karstification builds the primary pore framework; supergene karstification reconstructs and expands storage space via large-scale dissolution; and burial organic acid dissolution further upgrades reservoir quality. Their combined effects form extensive high-quality reservoirs and provide favorable storage conditions for subsequent hydrocarbon migration and accumulation. In addition, the regional unconformity formed at the end of the Dongwu Movement, together with fault-fracture systems generated by multi-stage tectonic movements, effectively connects high-quality source rocks of the underlying Longtan Formation with Changxing Formation reservoirs, creating favorable conditions for hydrocarbon migration and accumulation in the northeastern Sichuan Basin.

Quantitative evaluation using grey relational analysis indicates that among the three controlling factor categories, diagenesis contributes most to reservoir quality (correlation degree = 0.78), followed by sedimentary facies (0.69) and tectonic fractures (0.57). Specifically: dolomitization and dissolution intensity are the primary internal factors determining the preservation and upgrading of primary pores during deep burial; sedimentary microfacies define the upper limit of initial reservoir quality and control the spatial distribution framework of reservoirs; tectonic fractures mainly enhance permeability with limited contribution to total porosity, but are critical for high-yield wells in low-porosity reservoirs.

6 Conclusions

(1) The Changxing Formation reservoirs in the Huanglongchang Structure are typical platform-margin reef-shoal carbonate reservoirs. Reservoir lithologies are dominated by oolitic dolomite, reef breccia dolomite, and rudstone dolomite. Reservoir space comprises pores, vugs, and fractures, with secondary dissolution pores (intercrystalline, matrix, intragranular, and moldic dissolution pores) constituting the primary storage space. The reservoirs are characterized by low porosity and low permeability with strong heterogeneity: porosity mainly concentrates in 4%–12%, and permeability mostly ranges from 0.1 to 10 mD; locally developed fracture–vug systems can form relatively high-permeability intervals. The natural gas is typical thermogenic dry gas with high methane and extremely low heavy hydrocarbons. Formation water is predominantly $CaCl_2$ type with ultra-high TDS, reflecting a strongly closed accumulation environment. The gas reservoir is a normal-pressure to slightly overpressured system under a normal geothermal gradient.

(2) The sedimentary environment is the primary control on the macroscopic distribution and original physical properties of the reservoirs. Controlled by the Kaijiang-Liangping Trough, the study area develops platform-margin facies, and the platform-margin reef-shoal belt is the most favorable zone. Among microfacies, the back-reef shoal exhibits the best reservoir quality, followed by reef core, whereas the fore-reef ramp has the poorest properties. The high-energy back-reef shoal setting promotes well-developed primary intergranular pores, which facilitate subsequent diagenetic modification.

(3) Multi-stage diagenesis is the core factor improving reservoir quality. Penecontemporaneous evaporative pumping dolomitization and multi-stage burial dolomitization create a rigid intercrystalline pore framework that resists compaction and preserves deep-burial pore space. Syndepositional karstification, supergene karstification induced by the Dongwu Movement uplift, burial organic-acid dissolution, and TSR-related dissolution are superimposed to form abundant secondary dissolution pores and vugs, substantially expanding storage capacity. Conversely, compaction, pressure solution, and calcite cementation are the main destructive processes that reduce porosity.

(4) Multi-stage tectonism from the Yanshanian to Himalayan controls fracture development and distribution. Fracture systems act as critical seepage pathways and significantly enhance permeability. Fracture intensity is structurally heterogeneous: structural highs, fault flanks, fault tips, and inflection points define Class I fracture zones with the highest

density and connectivity; fold axes and structural slopes constitute Class II zones; structural limbs and stable areas correspond to Class III zones with weaker fracturing. The superimposed area of platform-margin reef-shoal bodies and structural highs exhibits optimal reservoir quality and represents the favorable target for future exploration and development.

(5) For exploration, the superimposed zone of platform-margin back-reef shoal microfacies and structural highs should be the primary target for high-quality reservoir prediction. Wells located on fault flanks and fold axes with intense fracturing are more likely to achieve high gas productivity. For development, the strong heterogeneity caused by sedimentary microfacies differentiation and uneven fracture distribution must be fully considered. Infill and horizontal wells should be arranged perpendicular to the dominant fracture strike to maximize controlled reserves and recovery. In low-permeability, poorly fractured intervals, acid fracturing can be applied to connect matrix pores with natural fractures.

Data Availability Statement

The data that support the findings of this study are available from the corresponding author upon reasonable request.

Funding

The authors thank the PetroChina Southwest Oil & Gas Field Company for providing core and well logging data.

Conflicts of Interest

The authors declare no conflicts of interest.

AI Use Statement

The authors declare that no generative AI was used in the preparation of this manuscript.

Ethical Approval and Consent to Participate

Not applicable.

References

[1] Wilson, J. L. (1976). Carbonate facies in geologic history. *Mineralogical Magazine*, 40(315), 804. [CrossRef]

[2] Schlager, W. (2005). *Carbonate Sedimentology and Sequence Stratigraphy* (Concepts in Sedimentology and Paleontology 8). SEPM. [CrossRef]

[3] Noyahr, C. V., Weissenberger, J. A., Harris, N. B., & Banks, J. (2023). A facies-and sequence stratigraphy-based reservoir model for a carbonate reef complex: South Swan Hills oil pool, Alberta. *Marine and Petroleum Geology, 152*, 106226. [CrossRef]

[4] Janjuhah, H. T., Salim, A. M. A., Alansari, A., & Ghosh, D. P. (2018). Presence of microporosity in Miocene carbonate platform, Central Luconia, offshore Sarawak, Malaysia. *Arabian Journal of Geosciences, 11*(9), 204. [CrossRef]

[5] Ma, Y., Zhang, S., Guo, T., Zhu, G., Cai, X., & Li, M. (2008). Petroleum geology of the Puguang sour gas field in the Sichuan Basin, SW China. *Marine and petroleum geology, 25*(4-5), 357-370. [CrossRef]

[6] Hong, H. T., Wang, Y. G., & Yang, T. Q. (2008). Sedimentary facies of Changxing Formation and distribution of organic reef gas reservoirs in northern Sichuan Basin. *Natural Gas Industry*, 28(1), 38-41. https://trqgy.paperonce.org/#/digest?ArticleID=3552

[7] Yongsheng, M. A., Chuanlong, M. O. U., Qinyin, T. A. N., Qian, Y. U., & Ruihua, W. A. N. G. (2007). Reef-bank features and their constraint to reservoirs of natural gas, from Permian Changxing Formation to Triassic Feixianguan Formation in Daxian-Xuanhan Area of Sichuan Province, South China. *Earth Science Frontiers, 14*(1), 182-192. [CrossRef]

[8] Ma, Y., Guo, X., Guo, T., Huang, R., Cai, X., & Li, G. (2007). The Puguang gas field: New giant discovery in the mature Sichuan Basin, southwest China. *AAPG bulletin, 91*(5), 627-643. [CrossRef]

[9] Wang, Y. S., Xu, M., Yang, Y. N., Xia, Q., Jiang, B., Yang, C., & Zhang, H. (2022). Structural characteristics and deformation evolution of an intra-continental fold-thrust belt in Eastern Sichuan: Insights into analogue sandbox models. *Frontiers in Earth Science, 10*, 897882. [CrossRef]

[10] Zuo, M., Wang, J., Sun, X., Hu, Z., Bai, Y., Yang, W., & Li, H. (2024). Platform margin belt structure and sedimentation characteristics of Changxing Formation reefs on both sides of the Kaijiang-Liangping trough, eastern Sichuan Basin, China. *Open Geosciences, 16*(1), 20220615. [CrossRef]

[11] Liu, D., Tang, Y., Yu, J., & Xie, F. (2006). Features of organic reefs in the Upper Permian Changxing Formation and prediction of hidden reefs in the Huanglongchang structure, eastern Sichuan. *Geology in China, 33*(2), 427-435. http://geochina.cgs.gov.cn/en/article/pdf/preview/20060222.pdf

[12] Zhang, B., Zheng, R., Wang, X., Zheng, C., Wen, H., Luo, Y., & Chi, Y. (2012). Geochemical characteristics and diagenetic systems of dolomite reservoirs of the Changxing Formation in the eastern Sichuan Basin, China. *Petroleum Science, 9*(2), 141-153. [CrossRef]

[13] Gu, Y., Jiang, Y., Fu, Y., Chen, Z., Zhang, J., Zhou, L., & Jiang, Z. (2019). Hydrocarbon accumulation and main controlling factors of reef-shoal gas reservoirs in Changxing Formation in the complex tectonic area, Eastern Sichuan Basin. *Arabian Journal of Geosciences, 12*(24), 776. [CrossRef]

[14] Zhao, H., Yi, J., Zhang, H., Zhao, R., Zhang, J., Dai, J., ... & An, H. (2024). Seismic geological characteristics and gas reservoir distribution of Changxing Formation biological bio-reef reservoir in the Longhuichang-Tieshan area, northeastern Sichuan Basin, China. *Journal of Natural Gas Geoscience, 9*(2), 111-122. [CrossRef]

[15] Li, Y., Wen, H. G., Xu, W. L., & Zhao, S.. (2019). Genesis of Changxing Formation dolomite in Huanglongchang area, northeastern Sichuan Basin. *Journal of Chengdu University of Technology: Science & Technology Edition, 46*(1), 41-52, 63. [CrossRef]

[16] Embry, A. F., & Klovan, J. E. (1971). A late Devonian reef tract on northeastern Banks Island, NWT. *Bulletin of Canadian petroleum geology, 19*(4), 730-781. [CrossRef]

[17] Lucia, F. J. (1995). Rock-fabric/petrophysical classification of carbonate pore space for reservoir characterization. *AAPG bulletin, 79*(9), 1275-1300. [CrossRef]

[18] Singh, K. H., & Joshi, R. M. (Eds.). (2020). *Petro-physics and Rock Physics of Carbonate Reservoirs*. Springer, Singapore. [CrossRef]

[19] Ellis, D. V., & Singer, J. M. (2008). *Well Logging for Earth Scientists* (2nd ed.). Springer, Dordrecht. [CrossRef]

[20] Bateman, R. M. (2012). *Openhole Log Analysis and Formation Evaluation* (2nd ed.). Society of Petroleum Engineers (SPE), Richardson, TX. [CrossRef]

[21] Barros Galvis, N. E. (2018). *Geomechanics, Fluid Dynamics and Well Testing, Applied to Naturally Fractured Carbonate Reservoirs*. Springer, Cham. [CrossRef]

[22] Long, W. E. N., Bing, L. U. O., Xiao, C. H. E. N., Wenzheng, L. I., Yifeng, L. I. U., Anping, H. U., & Anjiang, S. H. E. N. (2025). Formation and preservation of pores in deep limestone reservoirs: A case study of Upper Permian Changxing Formation, central Sichuan Basin, SW China. *Petroleum Exploration and Development, 52*(2), 330-345. [CrossRef]

[23] Tan, L., Liu, H., Tang, Y., Luo, B., Zhang, Y., Yang, Y., ... & Yang, X. (2020). Characteristics and mechanism of upper permian reef reservoirs in the Eastern Longgang area, Northeastern Sichuan Basin, China. *Petroleum, 6*(2), 130-137. [CrossRef]

[24] Machel, H. G. (2004). Concepts and models of dolomitization: a critical reappraisal. *Geological Society, London, Special Publications*, 235(1), 7-63. [CrossRef]

[25] Huang, S., Zhao, Z., Yue, A., Jiang, H., Tian, X., Jiang, Q., ... & Song, H. (2024). Differences in gas sources of the Changxing–Feixianguan formations around the Kaijiang-Liangping Trough and favorable exploration directions for coal-formed gas generated by the Upper Permian Longtan Formation, Sichuan Basin, China. *Journal of Natural Gas Geoscience, 9*(5), 321-331. [CrossRef]

[26] Li, H., Qin, Q. R., Zhang, B. J., Ge, X. Y., Hu, X., Fan, C. H., & Tang, H. M. (2020). Tectonic fracture formation and distribution in ultradeep marine carbonate gas reservoirs: A case study of the Maokou Formation in the Jiulongshan Gas Field, Sichuan Basin, Southwest China. *Energy & Fuels, 34*(11), 14132-14146. [CrossRef]

[27] Loucks, R. G. (1999). Paleocave carbonate reservoirs: Origins, burial-depth modifications, spatial complexity, and reservoir implications. *AAPG bulletin, 83*(11), 1795-1834. [CrossRef]

[28] Budd, D. A., Frost III, E. L., Huntington, K. W., & Allwardt, P. F. (2013). Syndepositional deformation features in high-relief carbonate platforms: long-lived conduits for diagenetic fluids. *Journal of Sedimentary Research, 83*(1), 12-36. [CrossRef]

[29] Wang, H., Zhou, Q., Zhou, W., Zhang, Y., & He, J. (2021). Carbonate platform reef-shoal reservoir architecture study and characteristic evaluation: A case of S field in Turkmenistan. *Energies, 15*(1), 226. [CrossRef]

Liao Pan is currently a Master's candidate in Geology at the School of Geoscience and Technology, Southwest Petroleum University, Chengdu, China, with research interests in carbonate reservoir characterization and reef-shoal sedimentology. (Email: 1426628944@qq.com)

Qirong Qin received his Ph.D. degree in Geological Engineering from Chengdu University of Technology, Chengdu, China, in 2000. He is currently a Professor and Doctoral Supervisor at the School of Geoscience and Technology, Southwest Petroleum University, Chengdu, China. His research interests include structural geology, tectonic fractures, and the exploration and development of oil and gas reservoirs. (Email: qqrong@swpu.edu.cn)

Shilin Wang received his Ph.D. degree in Mineral Resource Prospecting and Exploration from Southwest Petroleum University, Chengdu, China, in 2013. He is currently with the School of Geoscience and Technology, Southwest Petroleum University, and mainly engages in research on petroleum and natural gas exploration and development. (Email: ybybwsl@163.com)

Hening Li is currently a Master's candidate in Geological Resources and Geological Engineering at the School of Geoscience and Technology, Southwest Petroleum University, Chengdu, China, with research interests in carbonate reservoir geology and reservoir evaluation. (Email: 3372737832@qq.com)

Mei Luo is currently a Master's candidate in Geology at the School of Geoscience and Technology, Southwest Petroleum University, Chengdu, China, with research interests in carbonate sedimentology and reservoir characterization. (Email: 19923743130@163.com)